Modeling an EAF using Dynamic Material and Energy Balances

S. Matson, W. Fred Ramirez,
Campus Box 424 – Dept. Chem. Eng.
University of Colorado
Boulder, CO 80309
(303)492-8660

P. Safe
GCTx, Inc.
Suite 250
4950 N. O'Connor Rd.
Irving, TX 75062

November 16, 1998

1 Introduction

With the steel industry at its current competitive levels, any advantage a producer may realize is almost always worth the effort. Developing and using a model of the electric arc furnace (EAF) to optimize its operation can improve existing furnaces to the peak of their potential. Our research efforts at the University of Colorado are to develop a realistic mathematical EAF model in order to optimize it with respect to energy consumption, yield, and fourth hole off-gas composition.

The EAF model presented previously [3] has been modified and expanded in order to improve accuracy and computational efficiency. The changes to the model include: addition of oil flash-off, replacing the compound balance with an atom balance, inclusion of an energy balance, and using Gibbs free energy minimization for chemical equilibrium.

The article will describe the model and its modifications as well as general model behavior. Preliminary optimization results will conclude this article.

2 Previous Model

The dynamic EAF model is based upon the combination of material balances around two control volumes, chemical equilibrium with each control volume, and scrap melting.

2.1 Control Volumes & Material Balances

The model is based upon material balances on two control volumes present in the furnace. The bath control volume (BCV) includes the liquid bath, the slag layer, and a small amount of gas. The gas control volume (GCV) includes only the free-board gases of the furnace. The two control volumes are shown in figure 1.

Each control volume has its own streams for mass addition or removal. The BCV receives mass through scrap melting, carbon injection, oxygen lancing, and concentration-driven transfer from the GCV. The BCV releases mass through concentration-driven transfer from the GCV and convection caused by the carbon boil.

The GCV receives mass through burner operation, air infiltration, convection from the BCV, and concentration-driven transfer from the BCV. The GCV releases mass through the fourth hole and concentration-driven transfer.

Material balances are written for particular constituents inside of each control volume as ordinary differential equations (ODEs). Integration of the ODEs yields a profile of the mass in each control volume as a function of time.

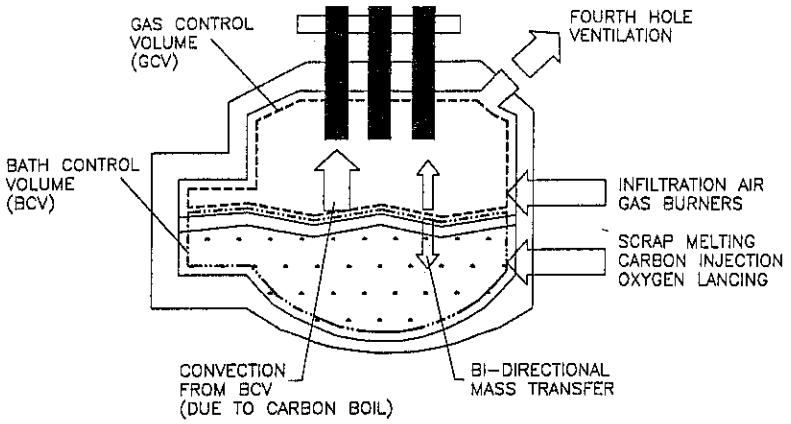

Figure 1: Furnace Model Control Volumes

2.2 Scrap Melting Model

The diverse scrap geometry requires simplifications in order to simulate its melting. The scrap is therefore assumed to be spherical and uniform. With this assumption, heat is applied to one sphere and the results are scaled up for the entire charge weight.

Energy not exiting the furnace or going to other sinks is applied to the exterior as the first boundary condition. The second boundary condition is temperature profile symmetry at the center of the sphere.

Two equations are used to describe the heat transfer. The transfer of sensible heat is described by a partial differential equation (PDE) in equation 1. The transfer of latent heat is described by an ordinary differential equation (ODE) in equation 2.

$$\frac{\partial T}{\partial t} = \frac{\alpha}{r^2}\frac{\partial}{\partial r}(r^2\frac{\partial T}{\partial r}) \tag{1}$$

T	temperature
t	time
r	radial distance
α	thermal diffusivity $k/(\rho C_p)$
ρ	density
C_p	heat capacity
k	thermal conductivity

As the sphere melts, the sphere radius varies as:

$$\frac{dR}{dt} = \frac{Energy\ Rate}{4\pi \cdot \Delta H_{melt} \cdot \rho_{solid} \cdot R^2} \tag{2}$$

R	outer sphere radius
t	time
$Energy\ Rate$	chemical and electrical energy
ΔH_{melt}	heat of fusion of steel
ρ_{solid}	density of solid scrap

The PDE (equation 1)is discretized in the space dimension, non-dimensionalized in space, and solved as an ODE. Heat is applied to the sphere until the melting temperature is reached, and then the melting ODE (equation 2) is used to decrease the sphere radius.

The melting model was first proposed by Matson and Ramirez [4].

2.3 Chemical Equilibrium

The assumption of equilibrium is reasonable since the system is high temperature and relatively well mixed. Chemical equilibrium eliminates the need to simulate rate limited chemical reactions which require extensive development of reaction networks and transport equations. A provision is made in the model to simulate transport limited reactions, however.

Because the real furnace contains a large number of compounds, a simplification must be made to keep the model computationally efficient. Each control volume contains only those compounds of interest or of high abundance. Figure 2 shows the compounds included in the model in their phases. Dissolved nitrogen ($\underline{N}$) and lime (CaO) have been added to bring the chemical model closer to reality.

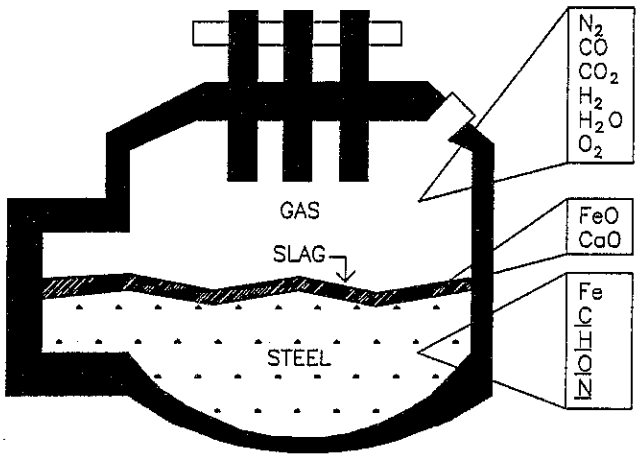

Figure 2: Furnace Compounds

3 Revised Model

3.1 Oil Flash-off

The EAF model is able to simulate the flashing of the organics (oil) that coat the scrap surface. A considerable amount of gas and energy is released just after charging due to the flashing and combustion of the coatings. These compounds contribute to the amount of combustibles present in the furnace free-board.

The release of these organics is closely tied to the scrap surface temperature. As the local surface temperature reaches the flash temperature of the organic, it is released into the gas. Physically it is impossible for all of the oil to be released instantaneously, so a time-dependent rate is defined for the model.

The model has been augmented to account for this release by adding one more term to the material balance that is coupled with the energy balance. Since the flashing phenomenon is related to the surface temperature of the scrap, the melting process is used.

After assuming a compound formula, flash time, and volatiles weight fraction, the flash rate can be determined by equation 3 which assumes a linearly decaying rate. The flash rate reaches zero at the end of the flash period.

$$F_{flash} = \begin{cases} -\frac{2M}{t_{flash}^2}(t_{charge} - t) + \frac{2M}{t_{flash}} & (t_{charge} < t < t_{charge} + t_{flash}) \\ 0.0 & (t > t_{charge} + t_{flash}) \end{cases} \quad (3)$$

F_{flash}	molar rate of oil addition to the GCV
M	total gram-moles of oil in charge
t_{flash}	flash-off duration
t_{charge}	time for the start of the charge
t	actual time in simulation

3.2 New Material Balance

The model now keeps material balances on the atoms, rather than the compounds, present in both of the control volumes. Using atoms in the material balance is advantageous since atoms are conserved in the EAF system. The balances on compounds are difficult to integrate because compounds are generated and consumed in reactions and therefore are not conserved.

As a direct result of this modification, flows into and out of each control volume must reflect atomic movement as determined by the movement of compounds. For example, if 1 mole/second of CO_2 is moving out of a control volume, then the carbon balance ODE shows a negative 1 mole/second and the oxygen balance shows a negative 2 mole/second rate of change for the flow terms.

Although the accounting is done with atoms, all other parts of the model continue to utilize the amounts of each which are always determined by a unique chemical equilibrium condition. Knowledge of the atomic population allows the calculation of the composition.

Table I shows the new atom balance ordinary differential equations. Most parameters are taken directly from furnace operating practice, but others are calculated from fundamental concepts. The calculated components are developed in table II.

The form of the new material balance equations reduce the number of ordinary differential equations from one per compound to one per atom type. The reduction of equations increases the computation speed while the atom balances are more stable to integrate than the compound balances.

3.3 Energy Balance

An energy balance is essential in a complete model of the EAF. Knowledge of the amounts and kinds of energy that pass into and out of the furnace is essential to make meaningful optimization results possible.

The energy balance tracks the total amount of sensible energy that enters and exits the system as well as the electrical energy input. The model contains temperature dependent heat capacity (C_p) data that is used to compute the energy contained of the flow streams.

Energy distribution within the furnace must be made somewhat arbitrarily to maintain model simplicity. Sinks for energy include: unmelted scrap, bath, water-cooled panels, and free-board gas sensible heat. With the energy sources and sinks identified and quantified, the model is able to predict the bath temperature after the melting of a charge is complete. Until melting is complete, the bath temperature is constant and the model puts energy into the unmelted scrap and other sinks.

Equation 4 is the energy accumulation ordinary differential equation for the EAF. During melting, the accumulated energy contributes to the sensible heat and latent heat. After melting is complete, the accumulated energy contributes to the sensible heat of the bath.

$$\frac{dE}{dt} = \sum H_i^{in} - \sum H_i^{out} + Q_{elec} - Q_{cool} \tag{4}$$

E	EAF system energy
H_i^{in}	rate of enthalpy gain due to material inflow
H_i^{out}	rate of enthalpy loss due to material outflow
Q_{elec}	rate electrical energy input
Q_{cool}	rate of cooling losses

Table I: New Atom Balance ODEs

Atom	Balance Equation
BCV	
C	$\frac{d}{dt}(N_C) = F_{inj} + \omega_C^{scrap} * F_{melt} * \frac{MW_C}{MW_{Fe}} - R_C - F_{out\ C}^{BCV}$
O	$\frac{d}{dt}(N_O) = 2F_{lance} - R_O - F_{out\ O}^{BCV}$
H	$\frac{d}{dt}(N_H) = -R_H - F_{out\ H}^{BCV}$
Fe	$\frac{d}{dt}(N_{Fe}) = F_{melt}$
N	$\frac{d}{dt}(N_N) = -R_N - F_{out\ N}^{BCV}$
GCV	
C	$\frac{d}{dt}(N_C) = F_{burner} - F_{out\ C}^{GCV} + F_{out\ C}^{BCV} + F_{flash}^{C} + R_C$
O	$\frac{d}{dt}(N_O) = 3F_{burner} + F_{spray} + 0.21 * 2 * F_{infil} - F_{out\ O}^{GCV} + F_{out\ O}^{BCV} + R_O$
H	$\frac{d}{dt}(N_H) = 2F_{burner} + 2F_{spray} - F_{out\ H}^{GCV} + F_{out\ H}^{BCV} + F_{flash}^{H} + R_H$
N	$\frac{d}{dt}(N_N) = 0.79 * 2 * F_{infil} - F_{out\ N}^{GCV} + F_{out\ N}^{BCV} + R_N$

N_i = number of i atoms in the control volume

MW_C = mol. wt. of carbon

MW_{Fe} = mol. wt. of iron

R_i = concentration driven molar flow of i atoms to the GCV (gmol/s)

F_{inj} = rate of carbon injection (gmol/s)

ω_C^{scrap} = wt. fraction carbon in scrap

F_{melt} = rate of melting (gmol/s)

F_{burner} = molar rate of methane flow to burner (gmol/s)

$F_{out\ i}^{XCV}$ = molar gas outflow rate of i out of the specified control volume(gmol/s)

F_{infil} = molar rate of air infiltration (gmol/s)

F_{lance} = molar rate of oxygen lancing (gmol/s)

F_{spray} = molar rate of water spray on electrode (gmol/s)

F_{flash}^{X} = molar rate of addition of X atoms due to flash-off (gmol/s)

Table II: Atom transfer relationships

Concentration Driven Mass Transfer	
$R_i = A \cdot k \cdot (y_i^{BCV} - y_i^{GCV})$	
A	Contact area between control volumes
k	Mass Transfer Coefficient
y_i^{XCV}	Mole fraction of compound i in the specified control volume
Total Convection Term from XCV	
$F_{out}^{XCV} = max(0,\ N_{gas}^{XCV} - N_{gas\ max}^{XCV})$	
$N_{gas}^{X}CV$	Total moles of gas in the specified control volume
$N_{gas\ max}^{XCV}$	Maximum moles allowed in specified control volume
Atomic Convection Term	
$F_{out\ i}^{XCV} = F_{out}^{XCV} \sum_{j=1}^{N} a_{ij} \cdot y_j$	
N	total number of compounds in control volume
a_{ij}	number of i atoms in j compound
y_j	mole fraction of j compound in control volume

The model assumes a reasonable off-gas temperature of 1800 K which sets the off-gas sensible energy. The cooling panel energy losses have been set arbitrarily to 65 kW-hr/ton. The remaining energy is divided between the slag and bath. Assuming bath and slag are the same temperature allows their temperature to be calculated.

The bath temperature is calculated from the cubic equation shown as equation 5.

$$T^3 + A \cdot T^2 + B \cdot T + C = 0 \tag{5}$$

$$A = \frac{\sum a_i N_i}{\sum b_i N_i/2}$$

$$B = \frac{-E - T_{ref} \sum a_i N_i - T_{ref}^2 \sum b_i N_i/2 + \sum c_i N_i/T_{ref}}{\sum b_i N_i/2}$$

$$C = -\frac{\sum c_i N_i}{b_i N_i/2}$$

T	temperature
E	total accumulated energy
T_{ref}	enthalpy reference temperature
N_i	moles of compound i
$H_i(T)$	$= (a_i(T - T_{ref}) + b_i(T^2 - T_{ref}^2)/2 - c_i(1/T - 1/T_{ref}))N_i$

The temperature is calculated using a root test and formula give by Press, et al. [5]. Mathematically, the equation has three possible solutions for the temperature. It is our finding, however, that two of them are consistently non-physical negative numbers.

By quantifying the energy content of material streams with other energy inputs the model is able to predict the final bath temperature. The total energy consumption also is derived from the energy balance results. Knowing the types and amounts of energy in the system aids in the development of new optimization strategies.

3.4 New Chemical Equilibrium Algorithm

In the previous model, the state of chemical equilibrium was described using a set of non-linear algebraic equilibrium equations. The solution of these equations determined the amounts of each compound present in a particular control volume.

Although this method is based on equilibrium data found in the literature, solutions are sometimes found with high iteration counts or not found at all. A more robust method of determining chemical equilibrium using the minimization of the Gibbs free energy of the system is now utilized.

The new equilibrium model, called the RAND algorithm, follows that developed by White, et. al. [7] and described by Smith and Missen [6]. The main idea behind this equilibrium technique is that at equilibrium the Gibbs free energy of the system is at a global minimum.

The equilibrium problem is as follows:

$$\begin{aligned} Find: \quad & \min G(\mathbf{n}) = \sum_{i=1}^{N} n_i \mu_i \\ subject\ to: \quad & \sum_{i=1}^{N} a_{ki} n_i = b_k \qquad k = 1, 2, ..., M \end{aligned} \tag{6}$$

where:

$G(\mathbf{n})$	total Gibbs energy of the system
$\mathbf{n}$	vector of molar amounts of each compound
μ_i	chemical potential of compound i
a_{ki}	number of k atoms in compound i
b_k	atomic population of the k atom
M	total number of different atoms

The EAF model assumes both control volumes are made up of phases which are ideal mixtures, which justifies the use of equation 7 for the chemical potential, μ_i. Values for the reference state chemical potential are taken from the *JANAF Tables* [1].

$$\mu_i \;=\; \mu_i^* + RT \ln x_i \tag{7}$$

where:

μ_i	chemical potential of compound i in the mixture
μ_i^*	chemical potential of compound i at a reference state
R	universal gas constant
T	system temperature
x_i	mole fraction of species i in its phase

Using the method of Lagrange multipliers, the constraints can be absorbed into the problem:

$$\mathcal{L}(\mathbf{n}, \lambda) \;=\; \sum_{i=1}^{N} n_i \mu_i + \sum_{k=1}^{M} \lambda_k (b_k - \sum_{i=1}^{N} a_{ki} n_i) \tag{8}$$

While the constraint equations remain the same, the equilibrium condition then becomes:

$$\frac{\mu_i^*}{RT} + \ln x_i - \sum_{k=1}^{M} \frac{\lambda_k}{RT} a_{ki} \;=\; 0 \qquad\qquad i \;=\; 1, 2, ..., N' \tag{9}$$

where:

λ_k	Lagrange multiplier for the k^{th} constraint equation
N'	number of non-inert compounds

The RAND algorithm linearizes equation 9 about an arbitrary solution $(\mathbf{n}^{(m)}, \lambda^{(m)})$ and then rearranges to form an $M + \pi$ dimensional linear algebra problem. (π is the number of phases present.) The minimum Gibbs energy is found in a few iterations. The reader should consult Smith and Missen [6] for details on the algorithm.

The current model is able to calculate equilibrium compositions for both the one-phase gas control volume (GCV) and the three-phase bath control volume (BCV). The model assumes that all phases are ideal solutions and the appropriate thermodynamic mixing rules apply. The previous chemical model assumed a two phase system of gas and liquid in the BCV. The current model uses a three phase system of gas, slag, and liquid in the BCV. The addition of the slag phase brings the model closer to the real furnace system since the mole fraction for iron oxide (FeO) in equation 7 will now be calculated for its separate phase.

The new chemical equilibrium algorithm makes it possible to add new compounds to the system without defining new chemical reactions. The new method is also more robust in finding the equilibrium composition than the previous equilibrium expression formulation.

4 Model Operation

Combining the material and energy balances with the melting model and the chemical equilibrium model results in the dynamic EAF model. The model is able to simulate all of the major furnace operations including: carbon injection, addition of carbon bags, oxygen lancing, electrical power input, and variable burner operations.

A model that is able to predict the outcome of one operating profile is of limited utility. Our modeling efforts focus upon making this dynamic model as general as possible in order to accommodate both simple operation modifications and technological changes in EAF steel manufacture.

Two concerns of EAF operators are the tap to tap time and the electrical energy usage. Decreasing the tap to tap time increases overall furnace productivity and reducing electrical consumption improves furnace economic efficiency. The tap to tap time can be decreased if the same amount of energy can be put into the furnace in a shorter time. Higher energy input rates can be achieved by increasing electrical or chemical power. Electrical power is generally more expensive, so efforts focus upon the chemical energy power. If more carbon monoxide can be combusted to carbon dioxide inside of the furnace, a chemical power increase may be realized. One additional consideration in EAF operation is the total gas flow rate down stream from the combustion gap. If a furnace can be designed of require less combustion air at the gap, a significant reduction in capital and operating expenses is realized. The downstream flow rate effects will be examined in a future study.

Taking these factors into consideration, a set of performance criteria have been chosen to measure the effectiveness of operating changes. The three criteria chosen are: CO/CO_2 ratio, iron yield, and final bath temperature. The CO/CO_2 ratio is a measure of the degree of combustion in the furnace. The higher the ratio, the more chemical energy is wasted. The iron yield is a measure of the efficiency of the melting process and is an indicator of the magnitude of the reducing conditions inside of the furnace. Extreme reducing conditions, when maintained throughout the heat, result in a higher yield. The final bath temperature is a reflection of the energy recovery. Since furnace operators generally always use the same final temperature, prediction of a higher than desired temperature indicates a possibility for reduction in either the tap to tap time or energy input.

4.1 Model Parameters

The model requires several parameters that are derived from the furnace geometry, furnace practice, or based more in theory. A list of parameters and their values is given in table III.

The gas volumes of each of the control volumes are two parameters that must be specified. The GCV volume ($N^{GCV}_{gas\ max}$) is calculated from the furnace free-board volume and is currently assumed to be $1,600\ ft^3$. The BCV volume ($N^{BCV}_{gas\ max}$) is calculated to be that of the bath since the bath has been observed to double in volume during carbon boil [2]. The BCV gas volume being used is $704\ ft^3$.

The mass transfer coefficient, k in table II, that is used to calculate the amount of gas moving between control volumes is a calibration parameter. It is most useful to examine its effects on the carbon monoxide levels in each control volume. If the coefficient is high, then there is a stronger tendency for oxygen to be transfered to the BCV from the GCV since the BCV never contains gaseous oxygen. A higher transfer of O_2 to the BCV results in a lower yield and a higher CO to CO_2 ratio since oxygen is driven out of the GCV. The model currently uses a value of $0.5\ gmol/s/ft^2$ for k.

The melting model requires a value for the equivalent scrap radius. A value of 20 cm is used for all simulations in this paper. The electrode consumption rate is taken to be a reasonable value of 4 $lb./ton$.

Figure 3 shows the furnace operations taking place in a typical model run.

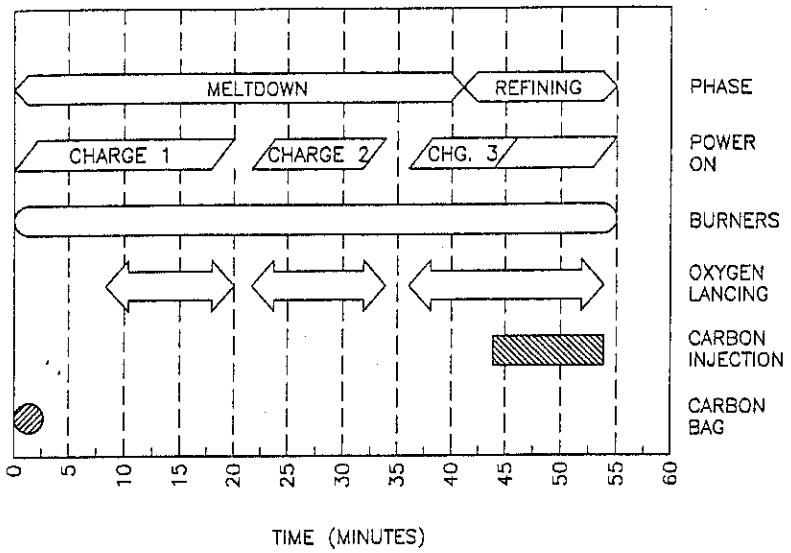

Figure 3: Furnace Operations

Table III: Parameter Values

Furnace & Operating Data	
Furnace Dia.	22'
Furnace Capacity	170 ton
Burner Rate	750 SCFM CH_4
O_2 Lancing Rate	2,200 SCFM
C Injection Rate	100 lb. /min.
C Bag Mass	5,000 lb.
Hot Heel Mass	10 ton

Other Parameters	
Air Infiltration Rate	17,500 SCFM
Scrap Equivalent Radius	20 cm
Exit Gas Temperature	1800 K
Hot Heel C content	0.1 $wt\%$
Scrap C Content	0.3 $wt\%$
Electrode Consumption Rate	4 $lb./ton$
Electrode Water Spray Rate	7.5 GPM

4.2 Results

Figure 4 shows the off-gas composition profile predicted for the base case parameters shown in figure 3 and table III. The flash-off period appears at the beginning of each charge as a declining peak of combustible gases. During flash-off, the conditions inside of the furnace are sufficiently deficient in oxygen to allow significant amounts of CO and H_2 to exist.

The step change in gas composition at the 7 minute mark is caused by the start of oxy-fuel burners. CO is the dominant component of the off-gas until the carbon is consumed at the 42 minute mark.

Figure 5 shows the bath temperature profile for the final minutes of the heat. Since melting has finished, the temperature rises linearly with time until the end of the heat.

Table IV summarizes the base case simulation results. The total CO and CO_2 are given as 127,750 SCF (standard cubic feet) and 135,820 SCF, respectively. The iron yield is 98.5% and the final bath temperature is $2,985^o F$.

4.2.1 Carbon Addition

The base case values for CO/CO_2, yield, and final temperature can be partially attributed to the rate of carbon and oxygen addition to the furnace. To illustrate this point, a simulation was performed that varied the rate of carbon addition from instantaneous (base case) to addition over the entire heat. During this exercise, the six factors of table IV were tracked. For each case, the same amount of carbon was added

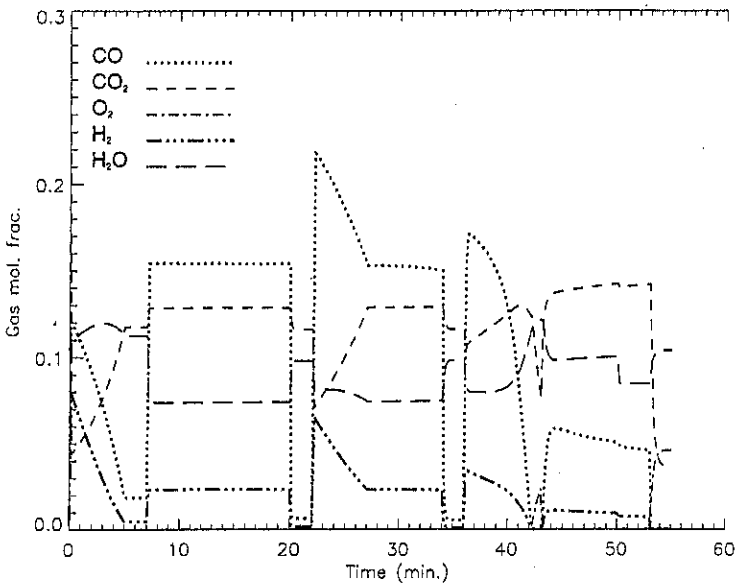

Figure 4: Base Case Off-Gas Composition

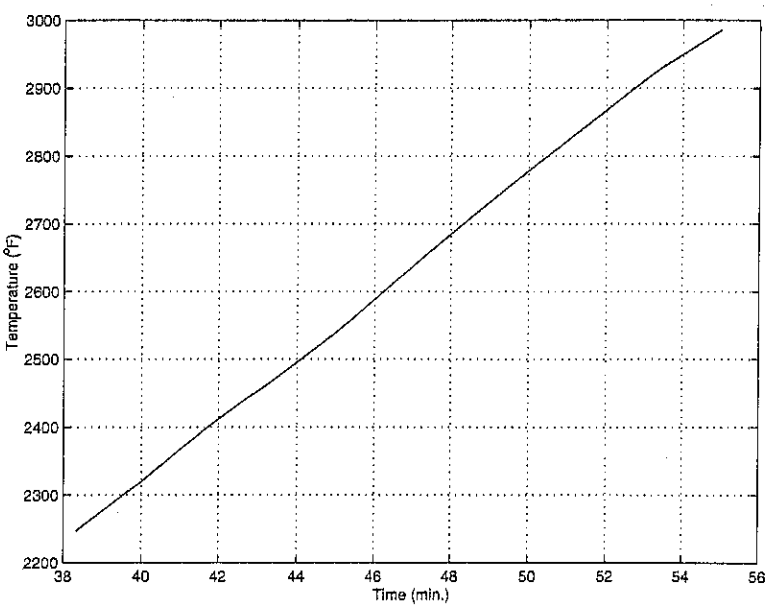

Figure 5: Temperature Profile at end of Heat

Table IV: Base Case Results Summary

Total CO released	127,750 SCF
Total CO_2 released	135,820 SCF
CO/CO_2	0.94
FeO	6.174 tons
Fe Yield	98.5%
Final Bath T	2985 °F

and the six factors of table IV were recorded.

Figure 6 gives the CO/CO_2 ratio for each carbon addition rate and shows that a critical time of 42 minutes exists for carbon addition. This time corresponds to the time that all of the carbon bag is consumed in the base case. If the carbon addition duration is above the critical time, the CO/CO_2 ratio decreases dramatically from the base case value and a higher degree of carbon combustion is achieved..

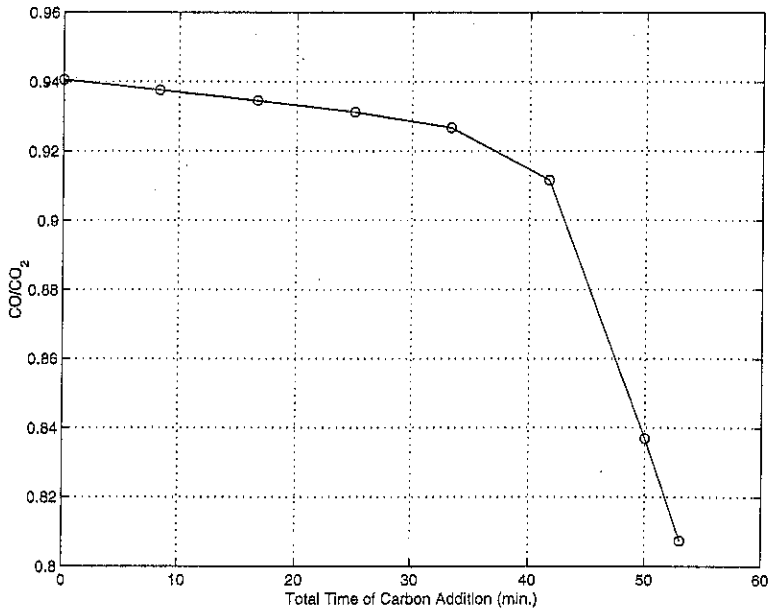

Figure 6: Effect of Varying Carbon Addition Rate on CO/CO_2

Figure 7 plots the amount of FeO present in the slag at the end of the heat for each carbon addition rate. This figure also exhibits the critical time of 42 minutes, after which the amount of oxide goes down and the yield goes up. The base case allows a more oxidizing condition to exist in the furnace after the carbon is consumed. Prolonging the carbon addition, maintains reducing conditions further into the heat and increases the yield.

The final bath temperature is given for each carbon addition rate in figure 8. After the critical time is exceeded, the final temperature rises to a higher value than the base case. It is unlikely that all of the energy released by the extra CO_2 production will reach the bath and increase the temperature. The figure therefore shows three separate curves that represent 20%, 40%, and 60% recovery of the combustion energy. The figure shows that even if 20% of this energy is recovered the model predicts a temperature increase of 10 degrees Fahrenheit.

4.2.2 Oxygen Addition

A study of varying amounts of oxygen addition, similar to the previous examination of carbon, has also been performed. Oxygen gas is introduced through the oxy-fuel burners in factors from 0 to 200% excess stoichiometric.

Figure 9 shows the effect of varying the amount of excess burner oxygen on the three results parameters of CO/CO_2, iron oxide, and final bath temperature.

The graphs show that as the excess oxygen is increased, the CO/CO_2 ratio decreases, the final temperature increases, and the iron oxide production increases. The final temperature predictions in the figure

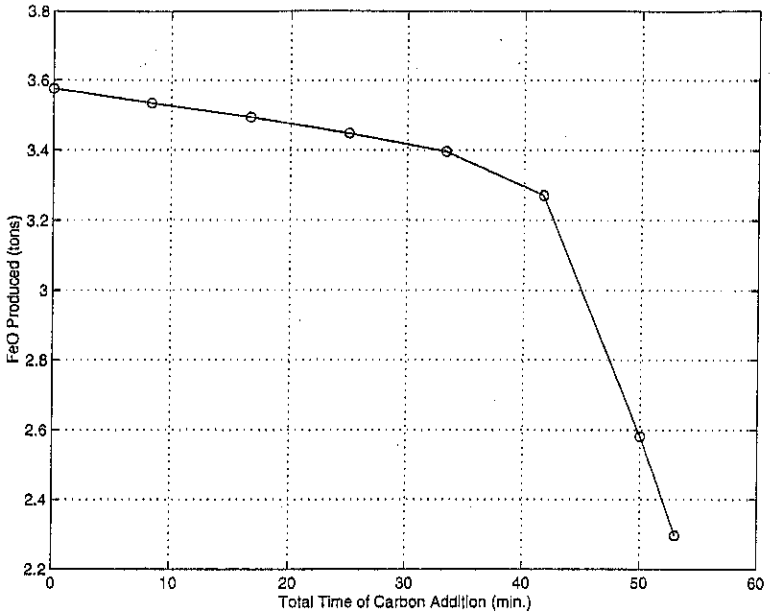

Figure 7: Effect of Varying Carbon Addition Rate on FeO Production

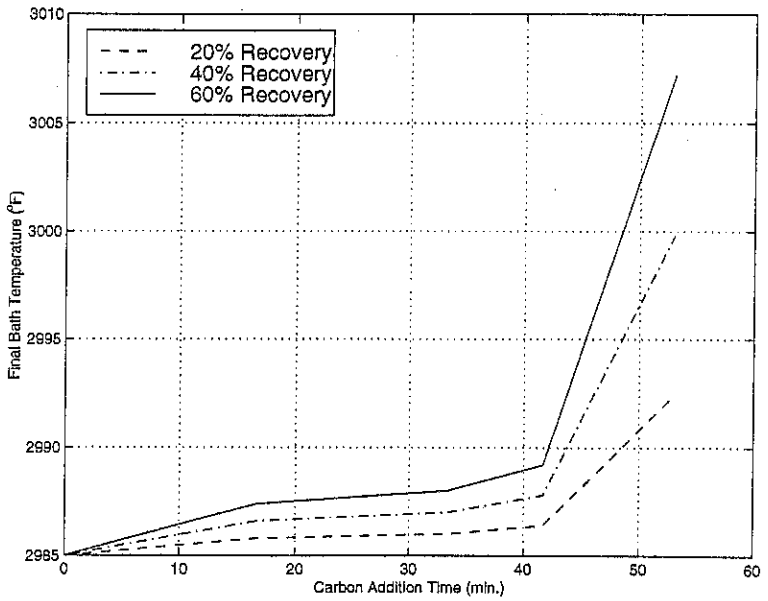

Figure 8: Effect of Varying Carbon Addition Rate on Final Bath Temperature

show fractional recoveries of 20, 40, and 60% as in the previous case. The effects are greater in magnitude than those for the carbon study for both the CO/CO_2 ratio and final temperature. In contrast to the carbon addition, the oxygen has a negative effect on the yield since it is promoting a more oxidizing environment for the bath.

4.2.3 Simultaneous Parameter Variation

A study has been undertaken to examine the effect of varying the carbon addition and oxygen addition simultaneously. Carbon addition and excess oxygen amounts were varied in the same ranges as the previous two studies. The results of these parameter combinations are shown in figure 10 as three three-dimensional plots. The figures show the effect of combining both of these operational changes. The left horizontal axis

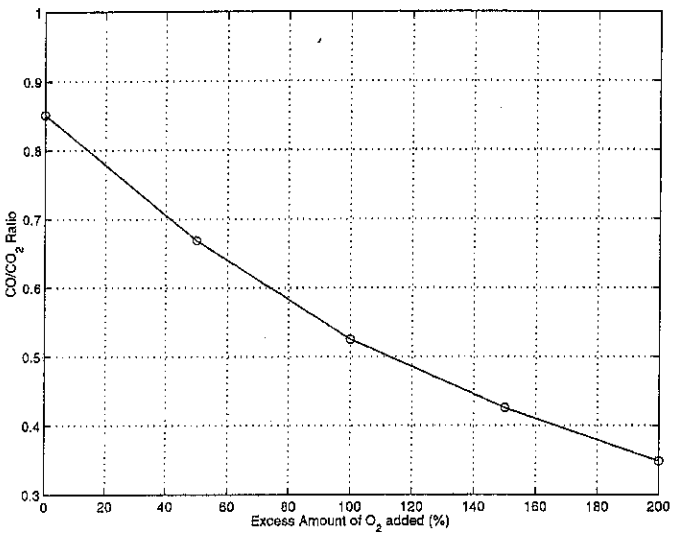

CO/CO_2 Effect

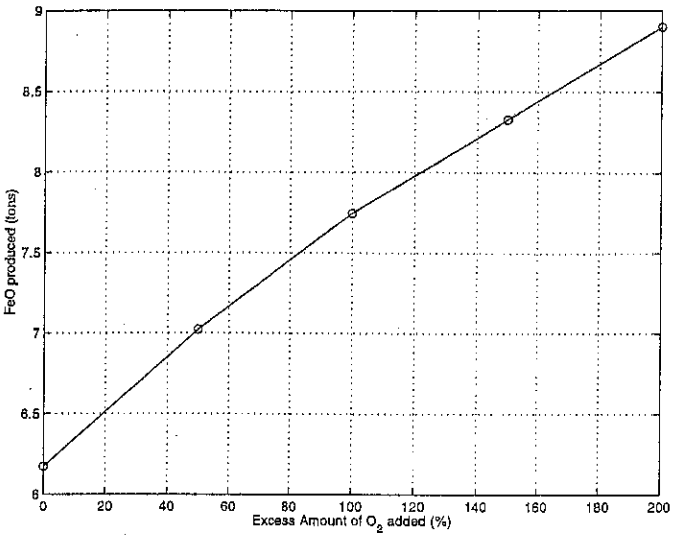

Iron Oxide Effect

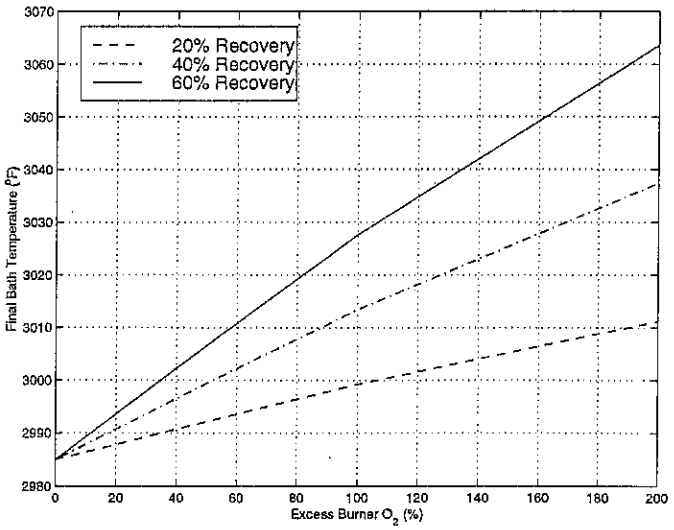

Final Bath Temperature

Figure 9: Excess O_2 Results

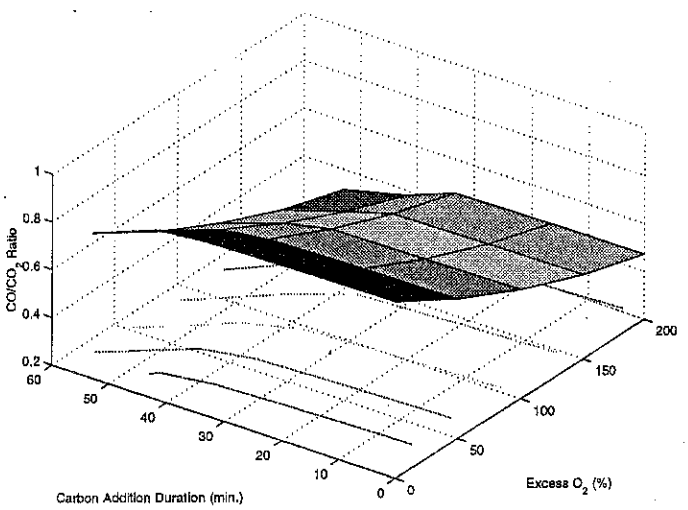

CO/CO_2 Effect

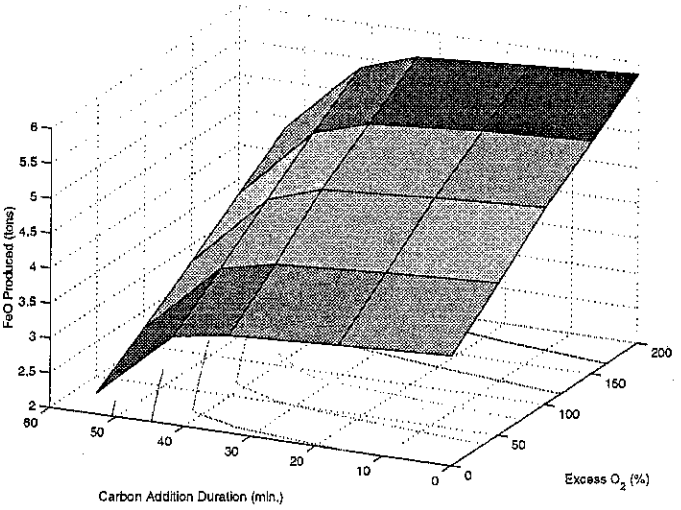

Iron Oxide Effect

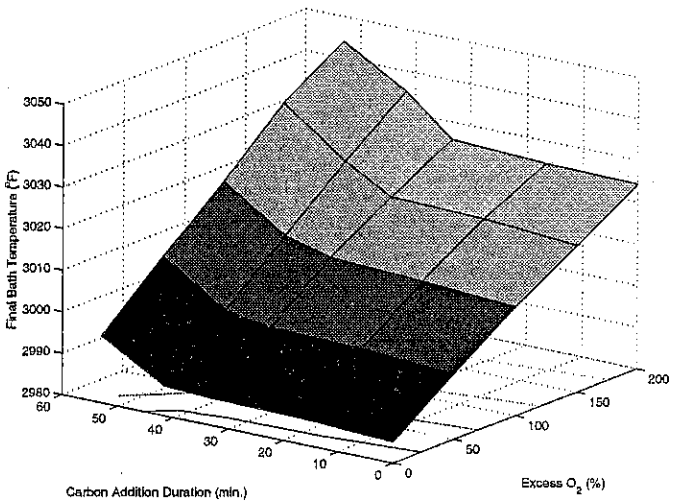

Final Bath Temperature Effect for 40% Recovery

Figure 10: Simultaneous Parameter Study Results

is the carbon addition duration and the right is excess oxygen percent. The vertical axis is given by the graph caption.

The CO/CO_2 graph predicts that the lowest ratio may be obtained when the carbon duration is as long as possible while the excess oxygen is 200%. The second graph predict the best yield is attained when the carbon addition is longest and the oxygen addition is zero.

5 Conclusions

An oil flash-off algorithm, Gibbs free energy minimization, energy balance, and atom balances are all new editions to the model. The flash-off algorithm was necessary to represent a real process that occurs in the furnace. The equilibrium routine and atom balances were added to improve model performance. The energy balances makes more detailed information available about the furnace.

A series of simulations showed that increasing the duration of reducing conditions in the furnace will increase yield, while lowering the carbon addition rate will decrease the CO/CO_2 ratio and increase the

final bath temperature.

Adding excess stoichiometric oxygen through the burners was also predicted to decrease the CO/CO_2 ratio and increase the bath temperature. The extra oxygen decreases the iron yield because it promotes oxidation of the bath.

Combining both modifications further improves the extent of carbon combustion and final bath temperature. The decrease in yield caused by adding extra oxygen can be countered to some extent by increasing the carbon addition duration.

References

[1] M.W. Chase and et. al. *JANAF Thermochemical Tables.* American Institute of Physics for the National Bureau of Standards, 3rd edition, 1986.

[2] W.T. Lankford and et al., editors. *The Making Shaping and Treating of Steel.* Herbick and Held, Pittsburgh, PA, 1985.

[3] S.A. Matson. The dynamic modeling of the electric arc furnace. Master's thesis, The University of Colorado at Boulder, Boulder, CO, December 1997.

[4] S.A. Matson and W.F. Ramirez. The dynamic modeling of an electric arc furnace. In *55th Electric Furnace Conference Proceedings.* Iron and Steel Society, November 1997.

[5] W.H. Press, S.A. Teukolsky, and et al. *Numerical Recipes in C.* Cambridge University Press, New York, NY, 1988.

[6] W.R. Smith and R.W. Missen. *Chemical Reaction Equilibrium Analysis: Theory and Algorithms.* Krieger Publishing Co., Malabar, FL, 1991.

[7] W.B. White, S.M Johnson, and G.B Dantzig. *J. Chem. Phys.*, 28:751, 1958.